Philippine Journal of Science
148 (S1): 199-209, Special Issue on Genomics
ISSN 0031 - 7683
Date Received: 19 Mar 2019

Characterization of the Biosynthetic Potential of the β-proteobacterium *Achromobacter xylosoxidans* Strain ISP2-142-O-2-A Using Microbiological, Chemical, and Genomic Approaches

Miguel Azcuna[1,2]*, Lilibeth Salvador-Reyes[1], Jortan Tun[1], Arturo Lluisma[1,3], Iris Diana Uy[1], Lovette Cunanan[1], Maria Auxilia Siringan[4], and Gisela P. Concepcion[1,3]

[1]The Marine Science Institute, University of the Philippines Diliman, Quezon City 1101 Philippines
[2]Verde Island Passage Center for Oceanographic Research and Aquatic Life Sciences, Batangas State University – ARASOF, Nasugbu, Batangas 4231 Philippines
[3]Philippine Genome Center, University of the Philippines Diliman, Quezon City 1101 Philippines
[4]Natural Science Research Center, University of the Philippines Diliman, Quezon City 1101 Philippines

This study characterized the biosynthetic potential of the bacterium *Achromobacter xylosoxidans* strain ISP2-142-O-2-A associated with the sponge *Haliclona* sp. nov. Chemistry- and bioactivity-guided purification of extracts from *A. xylosoxidans* afforded three compounds (1–3). The nucleoside 5'-deoxyadenosine (Compound 1) showed significant HIV cytoprotection activity with no cytotoxic activity to normal mammalian cells. The alkylquinolines 2-heptylquinolin-4-ol (Compound 2) and 2-nonylquinolin-4-ol (Compound 3) showed antimicrobial activity against *Staphylococcus aureus* and cytotoxicity to normal mammalian cells. This is the first report of Compounds 1–3 in *A. xylosoxidans*, and it is proposed that they have distinct roles for the bacterium to persist as a sponge-associated microorganism. Genomic analysis revealed the presence of 10 biosynthetic gene clusters (BGCs), indicating the potential of *A. xylosoxidans* strain ISP2-142-O-2-A as a source organism for other classes of bioactive natural products.

Keywords: alkylquinoline, antimicrobial, bacterial genome, biosynthetic gene clusters, marine natural products, nucleoside, sponge bacterial symbiosis

INTRODUCTION

The coral triangle located in the Indo-Pacific region is home to the most diverse sponge-assemblages in the world. Sponges are sessile filter feeders that provide the benthic framework of the coral reef ecosystem. Being the earliest multicellular organisms, they have well-defined layers of cellular organization, and their unique body structure is well adapted for filtering microorganisms from seawater (Santos-Gandelman *et al.* 2014). Sponges can host horizontally- or vertically-acquired microorganisms in their tissues (Lee *et al.* 2001). Microorganisms comprise 40–60% of the biomass of the sponge (Hentschel *et al.* 2006), and sponge microbial communities are composed of both specialists and generalists – with core microbiomes characterized by generalist symbionts with an under-representation of specialist symbionts (Thomas *et al.* 2015). These bacteria may be a source of nutrition or secondary metabolites for the sponge, with the latter functioning as allelochemicals that are useful for competition and evasion from spongivores. Indeed, symbiotic microorganisms are now regarded to be the true producers of the majority of secondary metabolites found in sponges. In the sponge *Theonella swinhoei*, the

*Corresponding Author: apachief@gmail.com

isolated bioactive compound onnamide was traced to the phylotypes *Candidatus Entotheonella factor* and *Candidatus Entotheonella gemina*, which are extensively distributed in this sponge (Bhushan *et al.* 2017, Piel *et al.* 2004).

Marine organisms are prolific sources of chemically diverse compounds and have been nicknamed 'blue gold' because of their potential for providing new drug leads. Microbial symbionts from marine invertebrates have contributed to as much as 80% of the novel antibiotics from the marine environment (Blockley *et al.* 2017). Marine microorganisms (MMOs) are beginning to occupy a central role in the discovery of new bioactive molecules (Perez and Fenical 2017).

The Philippine PharmaSeas Drug Discovery Program initiated the culture and biobanking of sponge-associated MMOs as source organisms of natural products for potential biomedical applications. A total of 739 MMOs were obtained in this program, and their crude extracts were screened for bioactivity against gram-positive and gram-negative pathogens and mammalian cancer cells. Following the screening, bioactive MMOs were characterized using microbiological, chemical, and genomic approaches. The bacterium ISP2-142-O-2-A, isolated from a *Haliclona* sp. nov. marine sponge from Agno, Pangasinan, Philippines was among the bioactive MMOs identified in this project. Here, we present the characterization of *Achromobacter xylosoxidans* strain ISP2-142-O-2-A and purification of bioactive compounds from this MMO. Genomic analysis was employed to identify the bacterium and reveal putative secondary metabolite BGCs to provide insights into the production of bioactive compounds that can be utilized as a guide for further drug discovery from this bacterium.

MATERIALS AND METHODS

Sponge Collection and Identification

The sponge was obtained from a collection site in Agno, Pangasinan, Philippines at a depth of 20 m. This particular sponge was intriguing because it was observed to be in competition with a neighboring coral. A sponge sample was obtained for spicule and section preparation (Figure I). Spicule forms, sizes, and their architecture – together with some morphological characters *e.g.*, color, shape, texture, surface, sizes of pores, *etc.* – were used in the identification of the sponge, as described in Longakit *et al.* 2005.

Isolation, Purification, and Characterization of the Bacterium from *Haliclona* sp. nov.

A tissue sample measuring 1 x 1 cm was placed in sterile seawater for microbial isolation. The sample was homogenized by maceration using a flame-sterilized mortar and pestle. The homogenate was serially diluted, and 100 µl of the 10^{-3} dilution was spread-plated onto ISP2 agar media. Agar plates were incubated at 27 ˚C for 90 d to allow sufficient growth of microorganisms. Isolation and purification were done once the microorganisms were fully grown. Plates were checked regularly to inspect for microbial growth, and sponge-associated microorganisms were purified by repeated streak plating. All purified microorganisms were cryopreserved using 20% glycerol at –80 ˚C.

The bacterium was subjected to preliminary taxonomic identification. 16S rRNA sequencing; Rapid Analytical Profile Index (API 20E, API20NE, BioMerieux, France); and BioLog tests were used to generate biochemical characteristics of taxonomic importance. Test results were encoded into the APIWEB™ software, and species determination was based on the similarity of the API profile of the bacterium to that of a genus or species in the API database. The BioLog MicroLog™ MicroStation with MicroLog™ Database software (California, USA) – on the other hand – was used to determine carbon utilization profiles. BioLog GN and GP microplate systems generated carbon utilization fingerprints that were compared to fingerprints in the database. Genus or species assignment was done if the fingerprint of the bacterium yielded percent probability that was greater than or equal to 50%. To examine morphological traits of the bacterium, pure cultures were sent to the Electron Microscopy Laboratory of the National Institute of Molecular Biology and Biotechnology, University of the Philippines Los Baños for examination of cellular traits with a scanning electron microscope (SEM), Jeol JSM-6301F, and transmission electron microscope (TEM), Hitachi H-300.

Purification of Bioactive Compounds from *A. xylosoxidans* Strain ISP2-142-O-2-A

Eight liters (8 L) of ISP2-142-O-2-A broth were cultured for three days or five days to produce Compounds 1 and 2–3, respectively in a shaking incubator (Daihan Wisecube, 27 ˚C, 150 rpm). On the day of harvest, HP-20 diaion resin (5% wt/vol) was added to the broth and incubated for 2 h. The resin was separated from the broth and washed sequentially with 100% distilled water (2000 mL); MeOH/water (1:3 v/v, 1000 mL); and 100% MeOH (2000 mL). The 100% MeOH crude extract was dried *in vacuo*. The 100% MeOH crude extract was further chromatographed on silica gel (Si-60 mesh size 70-230, Merck, 27 x 3.75 cm) under gravity column chromatography conditions using a step gradient of EtOAc in MeOH as follows: EtOAc 200 mL, EtOAc/MeOH (8:2 v/v) 200 mL, and EtOAc/MeOH (6:4 v/v) 200 mL (Figure II). The fraction labeled OCF 4-10, which eluted with 8:2 EtOAc: MeOH, was further purified by semipreparative HPLC using a Phenomenex Luna C18 column (250 x 10 mm), employing a gradient of 5–100% MeOH: water in

35 min to yield seven HPLC fractions (Figure IIIA). The fraction with t_R= 31.0 min was chromatographed using analytical HPLC on a Phenomenex Phenyl hexyl column (250 x 4.6 mm), employing a gradient of 5–100% MeOH: water in 35 min, to yield 5'-deoxyadenosine (Compound 1) (Figure IIIB). Fractions with t_R= 45.0 and 47.5 min were purified using analytical HPLC on a Phenomenex Phenyl hexyl column (250 x 4.6 mm), employing a gradient of 50–100% MeOH/water in 25 min, to yield 2-heptylquinolin-4-ol (Compound 2) and 2-nonylquinolin-4-ol (Compound 3) (Figures IIIC and IIID).

Chemical Characterization of Bioactive Compounds

Chemical characterization of all compounds was done by high-resolution mass spectrometry (MS) and 1D, 2D nuclear magnetic resonance (NMR) spectroscopy. Ultraviolet-visible (UV-Vis) absorbance was detected on a Shimadzu Prominence HPLC PDA detector. MS data were obtained using a QSTAR Elite QSTAR® XL Hybrid LC/MS/MS System (Applied Biosystems, Foster City, CA, USA) equipped with a turbo ion spray source delivering the sample at a rate of 40 µL/min. NMR spectroscopy data were obtained from a 500 MHz Varian NMR Spectrometer.

Biological Activity Evaluation

HIV cytoprotection. The HIV cytoprotection assay system was developed by (Chen *et al.* 1992) and adapted for screening by (Kiser *et al.* 1996). All cell lines and virus were acquired from the NIH AIDS Reagents Program. Briefly, 1A2 cells – a subclone of CEM-SS TART cells – were grown in Roswell Park Memorial Institute (RPMI) media supplemented with 10% (v/v) of fetal bovine serum (FBS), and 1% (v/v) of antibiotic and anti-mycotic were seeded in 96-well plates at a volume of 140 µL and a final density of 5000 cells/well. Subsequently, 50 µL of HIV-1 strain (HIV-$1_{MC99IIIB\Delta Tat\text{-}Rev}$) was added to the wells. Cells were treated with the compound at various concentrations in triplicates and incubated for 6 d at 37 ˚C in 5% CO_2. Cells infected with HIV-1 and treated with azidothymidine (AZT, US-NIH AIDS Reagents Program) (5 and 0.5 µg/mL) were used as the positive control, while cells infected with HIV-1 and cells without HIV-1 were used as negative controls. Cell viability was then assessed with a standard MTT assay adapted from Mossman (1983). Compounds that showed 50% cytoprotection ($p < 0.05$ using Students two-tailed t-test) relative to HIV-infected cells were considered active against HIV-1:

$$\%\ cytoprotection = \frac{(A_{sample} - A_{blank}) - (A_{HIV} - A_{blank})}{(A_{Control} - (A_{HIV} - A_{blank})} x\ 100\% \quad (1)$$

where A = absorbance at 570 nm.

HIV latency reactivation. JLAT 10.6 cells were maintained in RPMI 1640 medium supplemented with 10% (v/v) FBS, 0.45% (w/v) D-glucose, 0.01 mM sodium pyruvate, 0.15% (w/v) sodium bicarbonate, and penicillin-streptomycin. The cells were seeded in 96-well plates at a density of 5 x 10^5 cells/well. Cells were treated with the compounds at 50 µg/mL and 5 µg/mL and incubated for 48 h at 37 ˚C, 5% CO_2. Dimethysulfoxide (DMSO) (0.5%) was used as the negative control, while phorbol-12-myristate-13-acetate (PMA) (1 and 0.1 µg/mL) was used as the positive control. Fluorescence was measured by excitation at 485 nm and emission at 528 nm at 0 h and 48 h of treatment, and the fold reactivation was determined using the equation below. A fold-change of ≥ 2 was

$$\text{fold reactivation} = \frac{F\ sample}{F\ negative\ control}, \text{ where F = flourescence reading} \quad (2)$$

Antimicrobial activity. The protocol was based on the Clinical and Laboratory Standards Institute M7-A7 (CLSI 2006). Compounds 1–3 were tested for antimicrobial activity against *S. aureus* (ATCC 12600), methicillin-resistant *S. aureus* (MRSA) (ATCC 43300), *Kleibshella pneumoniae* (ATCC 13883), and *Pseudomonas aeruginosa* (ATCC 10145) with some modifications. Pathogen colonies were inoculated in 10 mL of cation-adjusted Mueller-Hinton broth (CAMHB, Pronadisa™) with 2% NaCl and incubated for 6 h at 37 ˚C, with shaking at 150 rpm. The turbidity of the bacterial suspension was adjusted with sterile broth to absorbance values of 0.08–0.1 at 625 nm to achieve a suspension containing approximately 1 x 10^8 CFU/mL. The adjusted inoculum was further diluted 100-fold and used for the assay. The inoculum was added to a 96-well plate containing 98 µL of CAMHB with 2% NaCl and 2 µL of each compound at concentrations of 10 and 100 µg/mL. The final density of the bacteria per well was approximately 5 x 10^5 CFU/mL. Afterward, the plate was sealed and incubated with shaking for 18–24 h at 37 ˚C. Finally, 20 µl of 0.02% resazurin was added into each well and the fluorescence signals were measured at 530 nm excitation and 590 nm emission using a microplate reader (Biotek Synergy™ HT). For positive controls, *S. aureus* and MRSA were treated with oxacillin (*S. aureus*: 0.1 µg/mL and 0.01 µg/mL; MRSA: 8 µg/mL and 4 µg/mL), while *K. pneumoniae* and *P. aeruginosa* were treated with nalidixic acid (*K. pneumoniae*: 8 µg/mL and 4 µg/mL; *P. aeruginosa*: 4 µg/mL and 2 µg/mL). The vehicle solvent was used as growth control. The results of the assays were expressed as % inhibition relative to the negative control using the following equation:

$$\%\ inhibition = (1 - \frac{absorbance\ treated - absorbance\ media}{absorbance\ vehicle - absorbance\ media}) x\ 100\% \quad (3)$$

Mammalian cytotoxicity. Compounds were tested for cytotoxic activity against the normal mammalian cell line MDCK (Madin-Darky canine kidney cells, ATCC® CCL-34) based on the protocol from Mosmann (1983) with modifications. MDCK was cultured in complete

minimal essential medium with Earles salts, 10% FBS, 2 mM L-glutamine, 1 mM sodium pyruvate, 1500 mg/L sodium bicarbonate, and 1% antibiotic-antimycotic (All from Gibco). The cells were grown in a CO_2 incubator (Nuaire™) at 37 ˚C and 5% CO_2.

Cells were seeded into a flat bottom 96 well-plate at a density of 1 x 10^4 cells/well in a volume of 200 µL and incubated at 37 ˚C for 24 h. Subsequently, cells were treated with the compounds at doses in half-log dilutions beginning at a concentration of 100 µg/mL. Doxorubicin (Sigma-Aldrich, 4 µg/mL and 0.4 µg/mL) was used as the positive control, and 1% DMSO was the vehicle control. The cells were incubated for 72 h at 37 ˚C, 5% CO_2. Afterward, the contents of the wells were discarded by sharp flicking the plate. Next, 15 µL of filtered MTT (5 mg/mL in 1X PBS) was added to each well and incubated at 37 ˚C, 5% CO_2 for 3 h. Finally, the formazan crystals formed from the reaction were solubilized with 100 µL of DMSO per well. After 5 min of shaking, the absorbance was read in a microplate reader (Biotek Synergy™ HT) at 570 nm. The assay results were expressed as percent cell death relative to the negative controls using the following equation:

$$\%\ cell\ death = \left(1 - \frac{absorbance\ treated - absorbance\ media}{absorbance\ vehicle - absorbance\ media}\right) x\ 100\% \quad (4)$$

Whole Genome Analysis of *A. xylosoxidans* Strain ISP2-142-O-2-A

DNA was isolated from 50 mL of a pure bacterium culture using QIAamp DNA Mini Kit (QIAGEN), Xanthogenate protocol (Tillet and Neilan 2000). The quality of genomic DNA from the extraction was analyzed through agarose gel electrophoresis, wherein genomic DNA that was not degraded appeared as a high molecular weight band with little or no smear in agarose gel.

The purified genomic DNA was sent to the Philippine Genome Center, University of the Philippines Diliman for sequencing using the Illumina MiSeq platform. Resulting NGS reads were used in the assembly together with the contigs generated by the PharmaSeas Drug Discovery Program - Project 5. Using the tools enumerated in Figure VI, pre-processing was carried out on MiSeq reads prior to assembly in order to remove low quality reads. Assembly was performed using SPAdes v3.10.0 and was assessed using QUAST v4.5.

Relevant features of the draft assembly were identified and annotated through Prokka v1.12 and Rapid Annotation using Subsystem Tool (RAST) v2.0. Prokka used external tools to predict salient features such as Prodigal for the prediction of coding sequences, RNAmmer for ribosomal RNA genes identification, Aragorn for transfer RNA genes, SignalP for signal leader peptides, and Infernal for non-coding RNAs identification. One of the outputs of Prokka is a GenBank file containing the sequences and annotations. This GenBank file was submitted to antiSMASH v5.0.0, SMURF, and PRISM for BGC prediction. The draft genome assembly in FastA format was also submitted to BAGEL3 for mining of bacteriocin encoding genes and other ribosomally synthesized and post-translationally-modified peptides.

Within the genes involved in the clusters of interest, a search for conserved domains was performed using NCBI CD-search and Pfam. Translated coding genes were searched against Swiss-Prot for sequence similarity to known proteins using Blast 2.3.0+ and Diamond v0.9.8.109. KEGG genes were identified using BlastKOALA v2.1, while eggNOG v4.5.1 was used to search for clusters of orthologous groups.

RESULTS

Biochemical Characterization, Morphological Analysis, and Phylogenetic Identification of the Bacterium from *Haliclona* sp. nov.

ISP2-142-O-2-A exhibited Gram-negative, slender to fusiform cells that are motile by peritrichous flagella (Figure 1). The cells measured 0.5–2.00 µm long and 0.25–0.75 µm wide. The bacterium was a catalase-positive microorganism that fermented glucose and reduced nitrate to nitrite. Both tryptophan and arginine were deaminated by the isolate, and it utilized citrate as a sole carbon source. Of the 19 enzymes studied, only acid phosphatase was produced. The isolate produced acid during the fermentation of D-galactose, mannose, xylose, and glucose.

With the BioLog system, 27 carbon sources were utilized by the bacterium: α-D-glucose; pyruvic acid methyl ester, succinic acid mono-methyl ester; cis-aconitic acid; citric acid; D-galactonic acid lactone; D-gluconic acid; ß-hydroxybutyric acid; itaconic acid; α-ketoglutaric acid; D;L-lactic acid; propionic acid; D-saccharic acid; sebacic acid; succinic acid; bromosuccinic acid; succinamic acid; D-alanine; L-alanyl-glycine; L-asparagine; L-aspartic acid; L-glutamic acid; glycyl-L-aspartic acid; L-phenylalanine; L-proline; L-pyroglutamic acid; and urocanic acid.

Based on the API and BioLog systems, the bacterium was identified as *Achromobacter xyloxosidans*, yielding high percent similarity (98.5% similarity) and high percent probability (95% probability). The 16S rRNA gene was extracted from the draft assembly using RNAmmer and was searched against the NCBI nucleotide database. The total length of the predicted 16S is 1,519 bp and the best

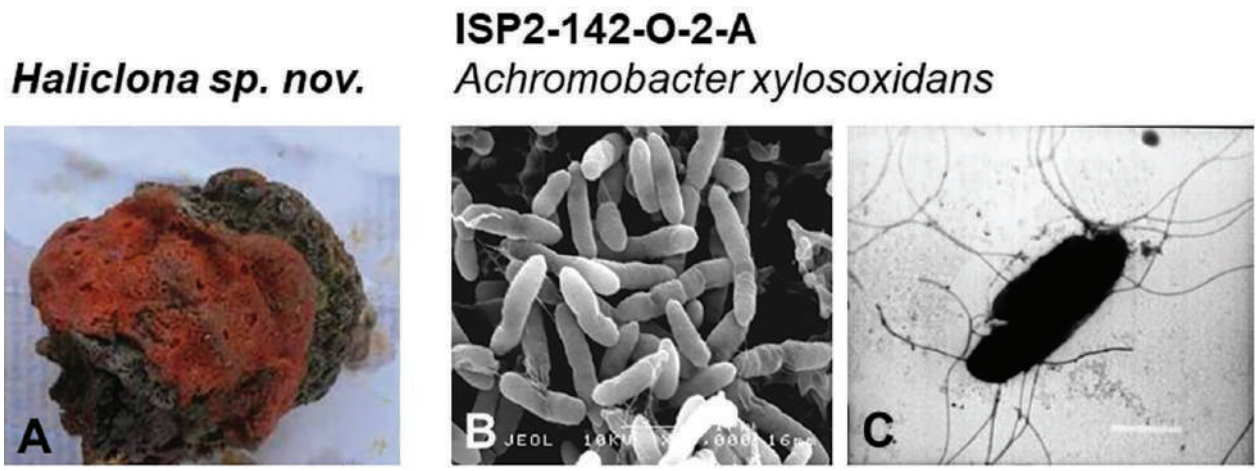

Figure 1. A – The bacterium was isolated from a bright orange *Haliclona* sp. nov. sponge in Agno, Pangasinan. B – SEM image showing the fusiform cells of the bacterium. C – TEM image showing the peritrichous flagella of the bacterium.

match was *A. xylosoxidans* strain FDAARGOS 162, among other *A. xylosoxidans* strains, all yielding 100% similarity.

Key differences were observed between ISP2-142-O-2-A and *A. xylosoxidans* reported in the literature. Firstly, the bacterium in this study was able to ferment glucose, while *A. xylosoxidans* was said to be strictly aerobic (Yabuuchi *et al.* 1974). Moreover, electron microscopy showed that ISP2-142-O-2-A had fusiform cells, which is different from the reported description of *A. xylosoxidans* having round-ended straight rods. However, a consistent feature of the bacterium in this study was its peritrichous flagella (Figure 1C), a typical characteristic of *A. xylosoxidans* (Yabuuchi *et al.* 1974).

Preliminary disk diffusion assays showed anti-*S. aureus* activity for the crude extract of the bacterium (Figure 2A). OCF 4-10 from open column chromatography was prioritized for HPLC purification of bioactive compounds since this fraction also showed anti-*S. aureus* activity in disk diffusion assays (Figure 2B). OCF 4-10 also contained several peaks with UV-Vis absorbances ranging 220–400 nm. Three HPLC fractions were pursued on the basis of biological activity and chemical profile.

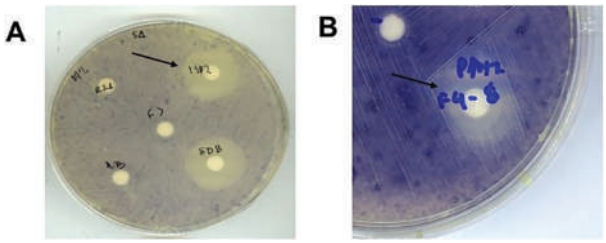

Figure 2. A – Anti-*S. aureus* activity of the crude extract of ISP2-142-O-2-A, with inhibition zone marked by the black arrow. B – Anti-*S. aureus* activity of OCF 4-10, with inhibition zone marked by the black arrow.

The HPLC fraction with t_R=31.0 min (Figure IIIA) did not show any antimicrobial activity against *S. aureus, K. pneumonia*, or *P. aeruginosa*. However, this was further pursued due to the presence of chemical signatures that are distinctive for antiviral agents. LC-HRESIMS gave a protonated molecule at m/z 252.1112 $[M+H]^+$, and was assigned a molecular formula of $C_{10}H_{13}N_5O_3$ with seven degrees of unsaturation. MSMS fragmentation yielded two major ions at m/z 136 and 119, which were assigned to adenine and deoxyribose fragments, respectively. Integration of the ^{1}H NMR signals indicated a total of 13 protons. The ^{1}H NMR spectrum showed three downfield aromatic protons (δ_H 8.31, 8.14, and 7.22 ppm); hydroxy protons (δ_H 5.44 and 5.17 ppm); methine protons (δ_H 5.84, 4.65, and 3.93 ppm); and a methyl group (δ_H 1.23 ppm). The structure of Compound 1 was elucidated as 5'-deoxyadenosine (Figure 3) based on HRMS, 1D, and 2D NMR data. Experimental values were in accordance with those reported in the literature (Westhof *et al.* 1977).

Anti-*S. aureus* activity was traced to the fractions with t_R= 45.0 and 47.5 min (Figure IIIA). The fraction with t_R= 45.0 min yielded 2-heptylquinolin-4-ol (Compound 2; Figure 3). The UV spectrum showed $_{max}$ at 236 nm and a doublet at 315 and 327 nm, which is characteristic for alkylquinolines (Royt *et al.* 2001). LC-HRESIMS gave a protonated molecule with m/z 244.1665 $[M+H]^+$ and was assigned a molecular formula of $C_{16}H_{21}NO$ with seven degrees of unsaturation. Dereplication using SciFinder (2019 version, American Chemical Society) resulted in one match, 2-heptylquinolin-4-ol, which was first reported as an antimicrobial metabolite from a marine pseudomonad (Wratten *et al.* 1977). UV-Vis, MS, and NMR data for Compound 2 were in agreement with that of the known compound 2-heptylquinolin-4-ol (Wratten *et al.* 1977).

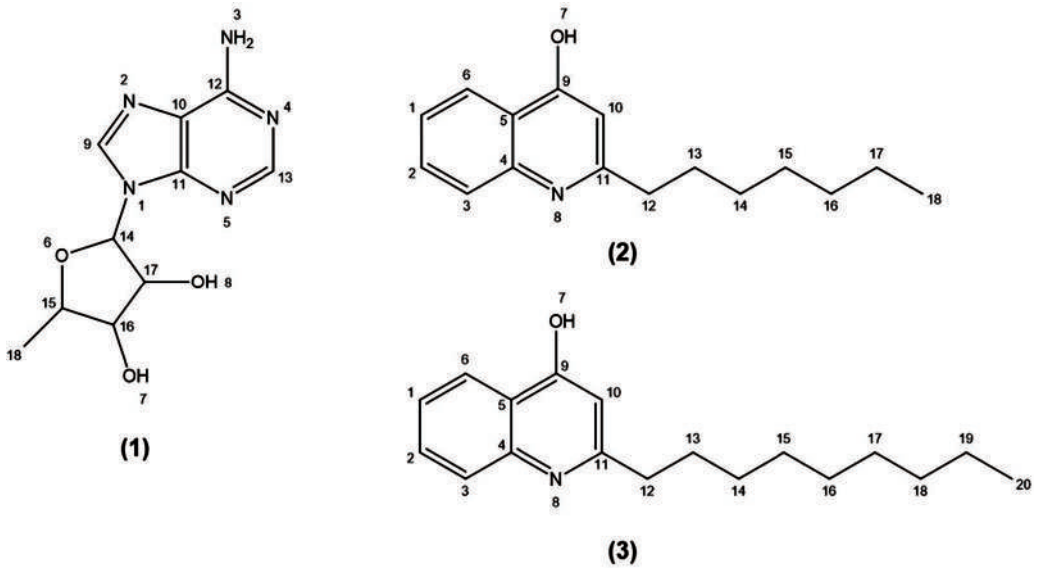

Figure 3. Purified compounds from *A. xylosoxidans* strain ISP2-142-O-2-A: 5'-deoxyadenosine, **(2)** 2-heptylquinolin-4-ol, and **(3)** 2-nonylquinolin-4-ol.

The fraction with t_R = 47.5 min afforded 2-nonylquinolin-4-ol (Compound 3; Figure 3). LC-HRESIMS showed a protonated peak at m/z 272.2058 $[M+H]^+$, indicating a difference of 28 Da from Compound 2. Molecular formula of $C_{18}H_{25}NO$ with seven degrees of unsaturation was assigned. The UV spectrum of Compound 3 showed a comparable profile with Compound 2, with λ_{max} at 236 nm and the doublet at 315 and 327 nm. Dereplication resulted in one match, 2-nonylquinolin-4-ol, which was reported as an antibacterial and cytotoxic compound from a sponge-associated pseudomonad (Bultel-Ponce *et al.* 1999). UV-Vis, MS, and NMR data for Compound 3 were in agreement with reported values (Royt *et al.* 2001) for 2-nonylquinolin-4-ol. Hence, Compound 3 bears the same moieties as Compound 2, except that it has an additional 2× CH_2 in the alkyl side chain.

Bioactivity Activity Evaluation

Compound 1 showed structural similarities with nucleoside reverse transcriptase inhibitors that are being used for HIV antiretroviral therapy. Hence, Compound 1 was tested for HIV cytoprotection and HIV latency reactivation assays. Significant activity was observed in the HIV cytoprotection assay at 0.5 and 0.05 µg/mL (Table 1 and Figure IVA). There was only a one-fold change in the HIV latency reactivation assay, indicating the absence of any significant activity (Table 1 and Figure IVB). Compound 1 did not show any cytotoxicity to MDCK cells at the same bioassay concentration (Table 1), suggesting that 5'-deoxyadenosine has a wide therapeutic window.

Compounds 2 and 3 showed significant anti-*S. aureus* activity with IC_{50} = 3 µg/mL and 1.55 µg/mL, respectively

Table 1. Summary of bioactivity testing of compounds isolated from *A. xylosoxidans*.

Compound	HIV cytoprotection (percent cell survival)	HIV latency reactivation (fold change)	IC_{50} MDCK cytotoxicity (µg/mL)	MIC *S. aureus* inhibition (µg/mL)
1	0.5 µg/mL = 68 ± 4 0.05 µg/mL = 45 ± 6	50 µg/mL = 1 5 µg/mL = 1	> 50	> 128
2	n/a	n/a	7.5	1.5
3	n/a	n/a	3.0	0.1
AZT	5 µg/mL = 100 ± 10 0.5 µg/mL = 94 ± 2	n/a	n/a	n/a
PMA	n/a	1 µg/mL= 3 0.1 µg/mL = 1.5	n/a	n/a
doxorubicin	n/a	n/a	0.1	n/a
oxacillin	n/a	n/a	n/a	0.5

n/a – not applicable

(Table 1, Figure V). There was no significant activity against methicillin-resistant *S.aureus*, *K. pneumoniae*, and *P. aeruginosa*. Compounds 2 and 3 showed cytotoxicity to MDCK cells with IC_{50} = 7.5 μg/mL and 3 μg/mL, respectively (Table 1 and Figure V). This indicates a narrow two-fold therapeutic window for 2-heptylquinolin-4-ol and 2-nonylquinolin-4-ol.

Genome Assembly, Protein Coding Sequence, and BGC Analysis of *A. xylosoxidans* Strain ISP2-142-O-2-A

Genomic sequencing of the bacterium showed that it had high percent similarity (100%) to *A. xylosoxidans* strain FDAARGOS 162 and many other *A. xylosoxidans* strains. Compared to *Achromobacter* genome assemblies available in NCBI, the draft assembly of ISP2-142-O-2-A covered 92.69% of the expected genome size. However, with 607 contigs, the assembly is said to be fragmented. Additional sequencing data, particularly long reads with large insert sizes, may improve the assembly. Table 2 shows the general features of the ISP2-142-O-2-A draft genome. Given that the assembly size of *A. xylosoxidans* in GenBank is approximately 6.8 Mbp, this assembly is nearly complete – with a size of 6,512,104 bp and N50 of 185,157 base pairs – taking account only of contigs with lengths greater than 500 bp.

A total of 5,969 protein-coding sequences were predicted by RAST wherein 50% were assigned with a subsystem category, while the rest of the proteins were not included in the subsystem. Figure 7 shows the number of predicted coding sequences involved in certain general functions. Proteins involved in the biosynthesis of amino acids were the most abundant, followed by proteins involved in carbohydrate metabolism and membrane transport.

Table 2. Summary of features of the *A. xylosoxidans* strain ISP2-142-O-2-A genome.

Genome size (bp)	6,512,104
Number of sequences	62
Number of contigs	607
Largest contig (bp)	609,559
N50 (bp)	185,157
Gap ratio (%)	0
G+C content	67.7
Protein coding genes	5,962
Average protein length	325.5
Percent coding region	89.4%
Non-coding region	10.6%
Structural RNAs	70
Ribosomal RNAs	4
16S	*1*
23S	*1*
5S	*2*
tRNA	66
RAST software	
Number of subsystems	503
Number of coding sequences	5,959
Genes in a subsystem	2,976
Non-hypothetical	*2,845*
Hypothetical	*131*
Genes not in a subsystem	2,983
Non-hypothetical	*1,751*
Hypothetical	*1,232*

A total of 10 BGCs were identified in the draft genome of the bacterium. These do not have any known homologous BGCs, which makes them potentially novel types of BGCs. The 10 novel BGCs were classified as the following types: siderophore, arylpolyene, terpene, two type-1 polyketide synthase, resorcinol, ectoine, phosphonate, betalactone, and one classified as 'other.' Genes encoding ectoine, a protective compound in osmotic stress conditions, were identified in one of the contigs. In addition, two siderophore clusters were predicted. No genes encoding for bacteriocins and post-translationally-modified peptides were observed.

The biosynthetic pathway of 2-heptylquinolin-4-ol and 2-nonylquinolin-4-ol and related 4-hydroxy-2-alkylquinolines (HAQ) in *P. aeruginosa* is directed via head-to-head condensation of the precursors anthranilic acid and beta-keto fatty acids (Brendenbruch *et al.* 2005). Anthranilic acid is known to be a common precursor of HAQ, and the *pqs*ABCDE biosynthetic cluster has been identified in *P. aeruginosa*. This *pqs*ABCDE operon codes for a putative coenzyme A ligase (*pqs*A); two beta-keto-acyl-acyl carrier protein synthases (*pqs*B, *pqs*C); and a *FabH1* homologous transacetylase (*pqs*D) – while *pqs*E encodes a response effector protein which is not involved in the biosynthesis of HAQ. Genomic sequencing of biosynthetic genes in *A. xylosoxidans* revealed genes that are identical or homologous to the abovementioned genes in *P. aeruginosa* (Table 3). Firstly, *trpE* and *trpG* genes – which function as anthranilate synthase components – were present in *A. xylosoxidans*. This suggests that the bacterium can produce anthranilic acid, the precursor of HAQ. Secondly, two genes with similar sequences to *pqs*A – 2-aminobenzoate-coenzyme A ligase (*abm*G) and benzoate-coenzyme A ligase – were present. The anthranilate and 2-aminobenzoate substrates for *pqs*A and *abm*G are nearly identical, except that 2-aminobenzoate lacks hydrogen in the carboxylic acid moiety. Thirdly, *FabH* and 3-oxoacyl-[acyl-carrier-protein] synthase III genes were found in *A. xylosoxidans*. These two genes possibly perform a similar function to the *pqsB* and *pqsC* genes, which function to synthesize 2-heptyl-4*(1H)*-quinolone and have a two-fold symmetry that mimics the *FabH* homodimer (Drees *et al.* 2016). However, the difference between *pqsC* and *FabH* lies in the active site of the former, which is approximately twice the volume of *FabH* enzymes. This excess volume may be a requirement to accommodate the aromatic substrate 2-aminobenzoylacetate. Therefore, it is uncertain if the

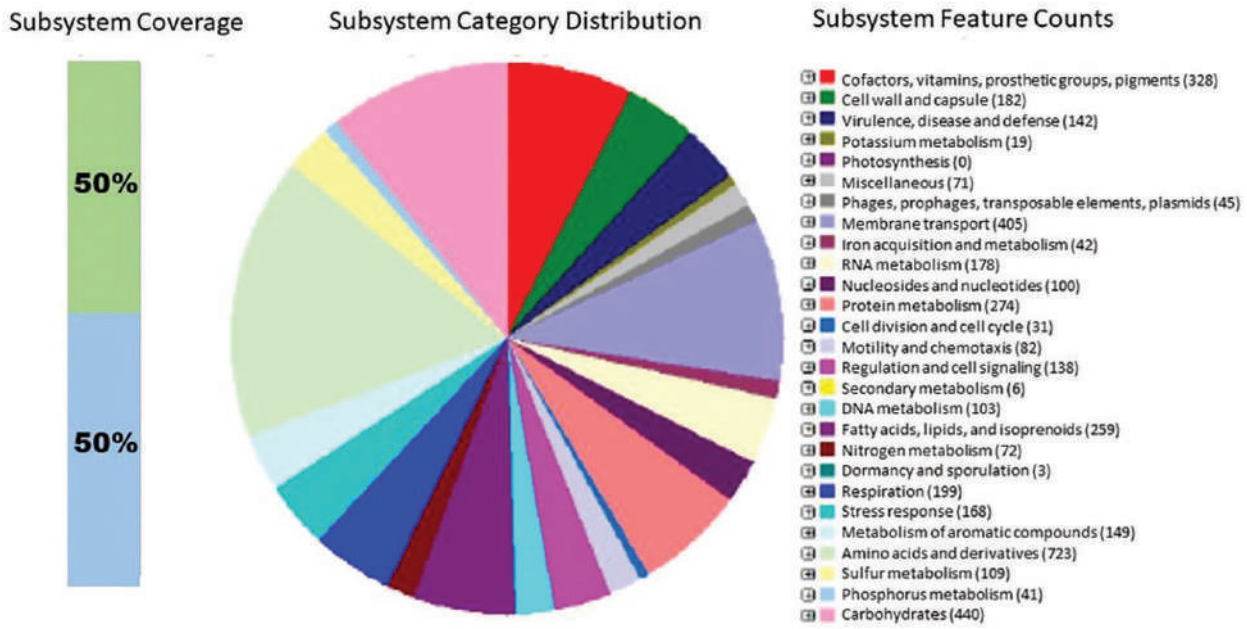

Figure 7. Classification of protein-coding sequences in ISP2-142-O-2-A according to general functions.

Table 3. Homologous genes found in *P. aeruginosa* (Brendenbruch *et al.* 2005, Bera *et al.* 2009, Drees *et al.* 2016) and *A. xylosoxidans* strain ISP2-142-O-2-A that are related to alkylquinoline production

***P. aeruginosa* gene**	***A. xylosoxidans* gene**	**Percent homology**	**Gene description**
trpE	*trpE*	24.70%	Anthranilate synthase component 1
trpG	*trpG*	63.15%	Anthranilate synthase component 2
pqsA	*abmG* (2-aminobenzoate coenzyme A ligase), benzoate CoA ligase	27.86%	Anthranilate coenzyme A ligase
pqsB, *pqsC*	*fabH*, 3-oxoacyl-[acyl carrier protein] synthase III	0%	Catalyzes the condensation of octanoyl-coenzyme A and 2-aminobenzoylacetate to form 2-heptyl-4*(1H)*-quinolone
pqsD	*fabH*, 3-oxoacyl-[acyl carrier protein] synthase III	20.30%	Catalyzes the condensation reaction between anthraniloyl-PqsD and malonyl-CoA or malonyl-ACP to form 2-aminobenzoylacetyl-CoA
pqsE	*tesA* thioesterase	0%	2-aminobenzoylacetyl-CoA thioesterase

active site of *FabH* can accommodate such a substrate. The aforementioned *FabH* and 3-oxoacyl-[acyl-carrier-protein] synthase III genes were also homologous to *pqsD*, which catalyzes a condensation reaction between anthraniloyl-PqsD and malonyl-CoA or malonyl-ACP. The difference between *FabH* and *pqsD* is that the latter is able to induce cyclization of PqsD-Protein-S-Anthraniloyl-L-Cystein to form 2-aminobenzoylacetyl-CoA (Bera *et al.* 2009). For *pqsE* – which is an aminobenzoylacetyl-CoA thioesterase – similar genes for thioesterases were found in *A. xylosoxidans*, specifically *tesA*. Hence, homologous genes related to the synthesis of HAQ were found in *A. xylosoxidans* strain ISP2-142-O-2-A, and this provides partial evidence for the biosynthetic production of alkylquinolines. Notably, the mechanisms in some genes (*e.g.*, *abmG, fabH, tesA*) were different from those in *P. aeruginosa*, with respect to active site structure or the required substrate.

DISCUSSION

In this paper, we report the characterization of the bacterium *A. xylosoxidans* strain ISP2-142-O-2-A using microbiological, chemical, and genomic approaches. Combination of chemistry- and bioactivity-guided

purification yielded three compounds. However, the genomic analysis only showed insights on the biosynthesis of the alkylquinolines. The software used for the BGC analysis, antiSMASH (Medema *et al.* 2011), employed the ClusterFinder algorithm to detect putative BGCs based on the assumption that biosynthetic pathways for unknown/unidentified compounds use the same enzyme families for the catalysis of vital chemical reactions seen in known compounds. ClusterFinder used the probabilistic method to predict BGC-like regions based on the rate of occurrence Pfam domains.

BGCs that yield a nucleoside like 5'-deoxyadenosine (Compound 1) were not observed in the genome of *A. xylosoxidans* strain ISP2-142-O-2-A. Compound 1 could be produced from a precursor-like adenosine that is enzymatically modified to remove the alcohol group at the 5'-position. A three enzyme metabolic pathway was proposed by Birmingham *et al.* (2014) for the biosynthesis of the nucleoside didanosine. Generally, 2,3-dideoxyribose 5-phosphate is generated by phosphorylation of 2,3-dideoxyribose by ribokinase and is converted to 2,3-dideoxyribose 1-phosphate using 1,5-phosphopentomutase. Finally, didanosine is generated by addition of hypoxanthine to 2,3-dideoxyribose 1-phosphate by purine nucleoside phosphorylase. Alternatively, Compound 1 can result from radical SAM pathway, but then this would result in 2'- or 3'-deoxygenation. In nature, a well-known nucleoside is 3'-deoxyadenosine or cordycepin from the fungus *Cordyceps militaris* (Cunningham *et al.* 1950).

This is the first report of the isolation of 2-heptylquinolin-4-ol (Compound 2) and 2-nonylquinolin-4-ol (Compound 3) from *A. xylosoxidans*, which is a beta-proteobacterium. Alkylquinolines have only been reported from gamma-proteobacteria like *Pseudomonas* spp. and *Alteromonas* sp. (Long *et al.* 2003, Bultel-Ponce *et al.* 1999). In *P. aeruginosa*, 2-heptylquinolin-4-ol serves as a precursor to the compound 2-heptyl-3-hydroxy-4(1H)-quinolone, a siderophore that acts as an iron scavenger (Diggle *et al.* 2007). Alkylquinolines in the sponge-associated *A. xylosoxidans* may be involved in iron sequestration to prevent iron toxicity in iron-rich environments (Royt *et al.* 2001). Alkylquinolines are also known to chelate iron (Nguyen *et al.* 2016). Alkylquinoline compounds produced by *A. xylosoxidans* may sequester iron from the microenvironment into their cell membranes, thereby making the iron unavailable to other cells and microorganisms. This sponge-associated bacterium could produce these types of compounds as a means of protection to ensure its survival in the sponge mesohyl, which is densely populated with marine viruses and bacteria.

Gamma-proteobacteria like *P. aeruginosa* are known to be dominant in sponge-microbe communities (Webster and Taylor 2012). Horizontal gene transfer from other bacteria (*e.g.*, *P. aeruginosa*) in the sponge holobiont may contribute to the ability of this strain of *A. xylosoxidans* to produce alkylquinolines. Beneficial mutations can occur in any part of the sponge holobiont, and microorganisms have short generation times. Such modifications can lead to phenotypic variation, upon which natural selection and genetic drift may operate (Webster and Thomas 2016).

The RAST prediction yielded a large percentage of protein-coding sequences for the metabolism of amino acids and membrane transport (Figure 7). This indicates that the bacterium has the capability to produce many types of compounds (*e.g.*, peptides) with amino acid backbone structures. As for membrane transport, the bacterium has been reported to transport iron through its membrane (Royt *et al.* 2001), and this could reflect the abundance of membrane transport coding sequences. Further research should aim to purify other classes of secondary metabolites with new or novel structural classes from this bacterium and address the presence of potentially cryptic compounds.

CONCLUSION

Secondary metabolites belonging to two structural classes were isolated from the sponge-associated β-proteobacterium *A. xylosoxidans* strain ISP2-142-O-2-A. The alkylquinolines 2-heptylquinolin-4-ol and 2-nonylquinolin-4-ol showed anti-*S. aureus* activity but showed cytotoxicity to normal mammalian cells. The nucleoside 5'-deoxyadenosine showed significant HIV cytoprotection activity with no cytotoxic activity to normal mammalian cells. Finally, the genomic analysis revealed 10 BGCs and a large percentage of protein-coding sequences related to amino acid metabolism, indicating that the bacterium is a potential source for the discovery of new bioactive compounds.

ACKNOWLEDGMENTS

We acknowledge funding from the Department of Science and Technology – Philippine Council of Agriculture, Aquatic and Natural Resources Research and Development and the Philippine Council for Health Research and Development through the PharmaSeas Drug Discovery Program and Discovery and Development of Health Products– Marine Component. We would like to thank Dr. Belinda Longakit for the taxonomic identification of the sponge. We also are grateful to the Philippine Mollusk Symbiont – International Cooperative Biodiversity Group for the HIV cytoprotection and HIV latency reactivation

assays. This study was done under the supervision of the Department of Agriculture – Bureau of Fisheries and Aquatic Resources, Philippines in compliance with the gratuitous permit requirements.

STATEMENT ON CONFLICT OF INTEREST

The authors declare no conflict of interest.

NOTES ON APPENDICES

The complete appendices section of the study is accessible at http://philjournsci.dost.gov.ph

REFERENCES

BERA AK, ATSANOVA V, ROBINSON H, EISENSTEIN E, COLEMAN JP, PESCI EC, PARSONS JF. 2009. Structure of PqsD, a *Pseudomonas* quinolone signal biosynthetic enzyme, in complex with anthranilate. Biochemistry 48: 8644–8655.

BIRMINGHAM WR, STARBIRD CA, PANOSIAN TD, NANNEMANN DP, IVERSON TM, BACHMANN BO. 2014. Biosynthetic construction of a didanosine biosynthetic pathway. Nat Chem Biol 10: 392–399.

BLOCKLEY A, ELLIOT DR, ROBERTS AP, SWEET M. 2017. Symbiotic microbes from marine invertebrates: Driving a new era of natural product drug discovery. Diversity 9: 1–13.

BRENDENBRUCH F, NIMTZ M, WRAY V, MORR M, MULLER R, HAUSSLER S. 2005. Biosynthetic pathway of *Pseudomonas aeruginosa* 4-hydroxy-2-alkylquinolines. J Bacteriol 187: 3630–3635.

BHUSHAN A, PETERS EE, PIEL J. 2017. *Entotheonella* bacteria as source of sponge-derived natural products: Opportunities for biotechnological production. In: Blue Biotechnology: Progress in Molecular and Subcellular Biology, Vol 55. Müller W, Schröder H, Wang X eds. Switzerland: Springer.

BULTEL-PONCE V, BERGE J, DEBITUS C, NICOLAS J, GUYOT M. 1999. Metabolites from the sponge associated bacterium *Pseudomonas* species. Mar Biotechnol 1: 384–390.

CHEN H, BOYLE TJ, MALIM MH, CULLEN BR, LYERLY HK. 1992. Derivation of a biologically contained replication system for human immunodeficiency virus type 1. Proc Natl Acad Sci USA 89: 7678–7682.

[CLSI] Clinical and Laboratory Standards Institute. 2006. Methods for Dilution Antimicrobial Susceptibility Tests for Bacteria That Grow Aerobically, Approved Standard – 7th ed. [CLSI document M7-A7; ISBN 1-56238-587-9]. Wayne, PA: CLSI.

CUNNINGHAM KG, MANSON W, SPRING FS, HUTCHINSON SA. 1950. Cordycepin, a metabolic product isolated from cultures of *Cordyceps militaris*. Nature 166: 949.

DIGGLE SP, MATTHIJS S, WRIGHT VJ, FLETCHER MP, CHHABRA SR, LAMONT IL, KONG X, HIDER RC, CORNELIS P, CAMARA M, WILLIAMS P. 2007. The *Pseudomonas aeruginosa* 4-quinolone signal molecules HHQ and PQS play multifunctional roles in quorum sensing and iron entrapment. Chem Biol 14: 87–96.

DREES SL, LI C, PRASETYA F, SALEEM M, DREVENY I, WILLIAMS P, HENNECKE U, EMSLEY J, FETZNER S. 2016. PqsBC, a condensing enzyme in the biosynthesis of the *Pseudomonas aeruginosa* quinolone signal. J Biol Chem 291: 6610–6624.

HENTSCHEL U, USHER KM, TAYLOR MW. 2006. Marine sponges as microbial fermenters. FEMS Microbiol Ecol 55: 167–177.

KISER R, MAKOVSKY S, TERPENING SJ, LAING N, CLANTON DJ. 1996. Assessment of a cytoprotection assay for the discovery and evaluation of anti-human immunodeficiency virus compounds utilizing a genetically-impaired virus. J Virol Methods 58: 99–109.

LEE YK, LEE J-H, LEE HK. 2001. Microbial symbiosis in marine sponges. J Microbiol 39: 254–256.

LONG RA, QURESHI A, FAULKNER DJ, AZAM F. 2003. 2-n-pentyl-4-quinolinol produced by a marine *Alteromonas* sp. and its potential ecological and biogeochemical roles. Appl Environ Microb 69: 568–576.

LONGAKIT BA, SOTTO FB, KELLY M. 2005. Shallow water marine sponges (Porifera) of Cebu, Philippines. *S*cience Diliman 17: 52–74.

MEDEMA MH, BLIN K, CIMERMANCIC P, DE JAGER V, ZAKRZEWSKI P, FISCHBACH MA, WEBER T, TAKANO E, BREITLING R. 2011. antiSMASH: Rapid annotation and analysis of secondary metabolite biosynthesis gene clusters in bacterial and fungal genome sequences. Nucleic Acids Research 39: W339–W346.

MOSMANN T. 1983. Rapid colorimetric assay for cellular growth and survival: Application to proliferation and cytotoxicity assays. J Immunol Methods 65: 55–63.

NGUYEN AT, JONES JW, CAMARA M, WILLIAMS P, KANE MA, OGLESBY-SHERROUSE AG. 2016. Cystic fibrosis isolates of *Pseudomonas aeruginosa* retain iron-regulated antimicrobial activity against *Staphylococcus aureus* through the action of multiple alkylquinolines. Frontiers in Microbiology 7: 1–13.

PEREZ LB, FENICAL W. 2017. Chapter 8 – Accessing marine microbial diversity for drug discovery. In: Microbial Resources: From Functional Existence in Nature to Applications. Kurtböke I ed. UK: Elsevier.

PIEL J, HUI D, WEN G, BUTZKE D, PLATZER M, FUSETANI N, MATSUNAGA S. 2004. Antitumor polyketide biosynthesis by an uncultivated bacterial symbiont of the marine sponge *Theonella swinhoei*. PNAS 101: 16222–16227.

ROYT PW, HONEYCHUCK RV, RAVICH V, PONNALURI P, PANNELL LK, BUYER JS, CHANDHOKE V, STALICK WM, DESESSO LC, DONOHUE S, GHEI R, RELYEA JD, RUIZ R. 2001. 4-hydroxy-2-nonylquinoline: A novel iron chelator isolated from a bacterial cell membrane. Bioorg Chem 29: 387–397.

SANTOS-GANDELMAN JF, GIAMBAGI-DEMARVAL M, OELEMANN WMR, LAPORT MS. 2014. Biotechnological potential of sponge-associated bacteria. Curr Pharm Biotechno 15: 143–155.

TILLET D, NEILAN BA. 2000. Xanthogenate nucleic acid isolation from cultured and environmental cyanobacteria. Journal of Phycology 36(1): 251–258.

THOMAS T, MOITINHO-SILVA L, LURGI M, BJORK JR, EASSON C, ASTUDILLO-GARCIA C, OLSON JB, ERWIN PM, LOPEX-LEGENTIL S, LUTER H, CHEVES-FONNEGRA A, COSTA R, SCHUPP PJ, STEINDLER L, ERPENBECK D, GILBERT J, KNIGHT R, ACKERMANN G, LOPEZ JV, TAYLOR MW, THACKER RW, MONTOYA JM, HENTSCHEL U, WEBSTER NS. 2015. Diversity, structure and convergent evolution of the global sponge microbiome. Nat Commun 7: 11870.

WEBSTER NS, TAYLOR MWY. 2012. Marine sponges and their microbial symbionts: Love and other relationships. Environ Microbiol 14: 335–346.

WEBSTER NS, THOMAS T. 2016. The sponge hologenome. American Society for Microbiology 7: 1–14.

WESTHOF E, PLACH H, CUNO I, LUDEMANN H-D. 1977. Proton magnetic resonance studies of 2'-, 3'-, and 5'-deoxyadenosine conformations in solution. Nucleic Acids Research 4(4): 939–953.

WRATTEN SJ, WOLFE MS, ANDERSEN RJ, FAULKNER DJ. 1977. Antibiotic metabolites from a marine pseudomonad. Antimicrob Agents Ch 11: 411–414.

YABUUCHI E, YANO I, GOTO S, TANIMURA E, ITO T, OHYAMA A. 1974. Description of *Achromobacter xylosoxidans* Yabuuchi and Ohyama 1971. Int J Syst Bacteriol 24: 470–477.

Table I. 1D and 2D NMR for compound (1) (500 MHz, DMSO-d$_6$).

Atom number	HSQC correlations δ_C (ppm)	δ_H (ppm, mult, *J* in Hz)	COSY correlations	HMBC correlations
1	–	–	–	–
2	153.07	8.31, s, 1H	–	4,5
3	–	–	–	–
4	150.00	–	–	–
5	119.51	–	–	–
6	156.50	–	–	–
6 – NH_2	–	7.22, s, 2H	–	5
7	–	–	–	–
8	140.28	8.14, s, 1H	–	2,4,6
9	–	–	–	–
1’	88.19	5.84, d, 1H	2’-H	–
2’	73.44	4.65, t, 1H	1’-H, 3’-H	–
2’ – OH	–	5.17, bs, 1H	4’-H	–
3’	73.44	4.65, t, 1H	2’-H, 3’-OH, 4’-H	–
3’ – OH	–	5.44, bs, 1H	3’-H	–
4’	81.23	3.93, m, 1H	3’-H, 5’-H	–
5’	19.27	1.23, d, 3H	4’-H	–

Table II. 1D and 2D NMR for compound (2) (500 MHz, DMSO-d$_6$).

Atom number	HSQC correlations δ_C (ppm)	δ_H (ppm, mult, *J* in Hz)	COSY correlations	HMBC correlations
1	122.97	7.25 (t, 1H, 8 Hz, 4Hz)	2-H, 6-H	2, 3, 6
2	131.79	7.59 (t, 1H)	1-H, 6-H	4, 6
3	118.55	7.53 (D, 1H)	2-H	1
4	140.80	–	–	–
5	118.55	–	–	–
6	125.09	8.02 (dd, 1H, 10 Hz)	1-H, 3-H	2, 4, 9
7 – OH	–	Not detected	–	–
8 – N	–	–	–	–
9	177.05	–	–	–
10	107.99	5.91 (s, 1H)	–	6, 11, 12
11	154.08	–	–	–
12	33.81	2.57 (t, 2H)	13-H	10, 11, 13
13	28.77	1.64 (t, 2H)	12-H, 14-H	11, 12, 14
14	28.83	1.28 (2H)	13-H, 15-H	13, 15
15	28.83	1.28 (2H)	14-H, 16-H	14, 16
16	31.58	1.25 (2H)	15-H, 17-H	15, 17, 18
17	22.45	1.25 (2H)	17-H. 18-H	15, 16, 18
18	14.35	0.85 (3H)	17-H	16, 17

Table III. 1D and 2D NMR for compound (3) (500 MHz, DMSO-d_6).

Atom number	HSQC correlations δ_C (ppm)	δ_H (ppm, mult, *J* in Hz)	COSY correlations	HMBC correlations
1	123.21	7.25 (t, 1H, 8 Hz, 4Hz)	2-H, 6-H	2, 3, 6
2	132.06	7.58 (t, 1H)	1-H, 6-H	4, 6
3	118.29	7.49 (d, 1H)	2-H	1
4	140.57	–	–	–
5	118.32	–	–	–
6	125.20	8.01 (d, 1H, 8 Hz)	1-H, 2-H	2, 4, 9
7 – OH	–	11.36 (br s, 1H)	–	–
8 – N	–	–	–	–
9	177.30	–	–	–
10	107.92	5.89 (s, 1H)	–	6, 11, 12
11	154.05	–	–	–
12	33.40	2.56 (t, 2H)	13-H	10, 11, 13
13	28.70	1.64 (t, 2H)	12-H, 14-H	14
14	28.96	1.28 (2H)	13-H, 15-H	13, 15
15	28.96	1.28 (2H)	14-H, 16-H	14, 16
16	28.96	1.28 (2H)	15-H, 17-H	15, 17
17	28.96	1.28 (2H)	16-H, 18-H	16, 18
18	31.65	1.28 (2H)	17-H, 19-H	17, 19
19	22.51	1.28 (2H)	18-H. 20-H	17, 18, 20
20	14.50	0.88 (3H)	19-H	18, 19

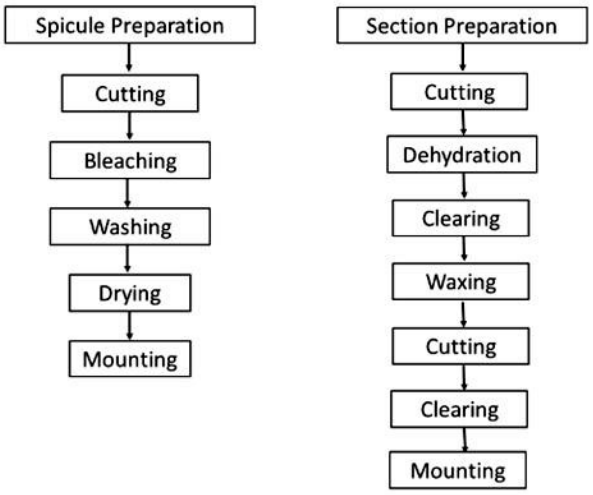

Figure I. Preparation of permanent slides used in the microscopic analysis of the sponge collected in Agno, Pangasinan, Philippines (taken from Longakit *et al.* 2005).

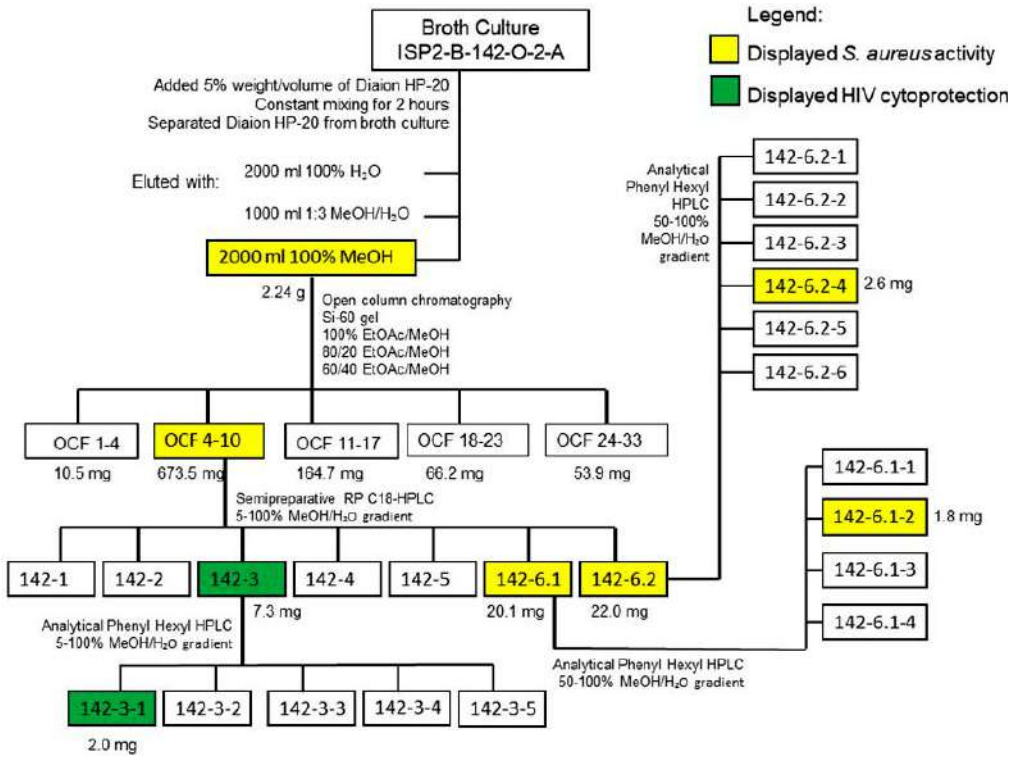

Figure II. The purification scheme of bioactive compounds from *A. xylosoxidans* strain ISP2-B-142-O-2-A.

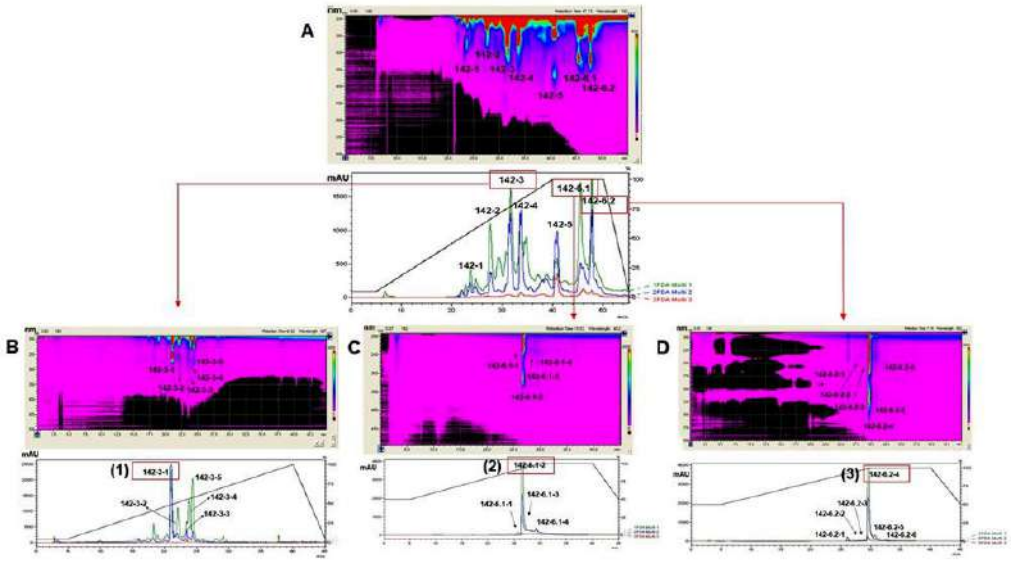

Figure III. A – HPLC UV-vis contour plot and chromatogram of OCF 4-10; luna C18 column: 250 x 10 mm; methanol-water gradient: 5–100% in 35 min; flow rate: 2 mL/ min; injection volume: 200 µL. B – HPLC UV-vis contour plot and chromatogram of 142-3; phenyl-hexyl column: 250 x 4.6 mm; methanol-water gradient: 5–100% in 35 min; flow rate: 1 mL/ min; injection volume: 50 µL. C – HPLC UV-vis contour plot and chromatogram of 142-6.1, showing the four HPLC fractions; phenyl-hexyl analytical column: 250 x 4.6 mm; methanol/water gradient: 50–100% in 25 min; flow rate: 1 mL/ min; injection volume: 30 µL. D – HPLC UV-vis contour plot (A) and chromatogram (B) of 142-6.2, showing the six HPLC fractions; phenyl-hexyl analytical column: 250 x 4.6 mm; methanol/water gradient: 50–100% in 25 min; flow rate: 1 mL/ min; injection volume: 30 µL; PDA detection wavelength: 220 nm (green), 254 nm (blue), and 360 nm (red).

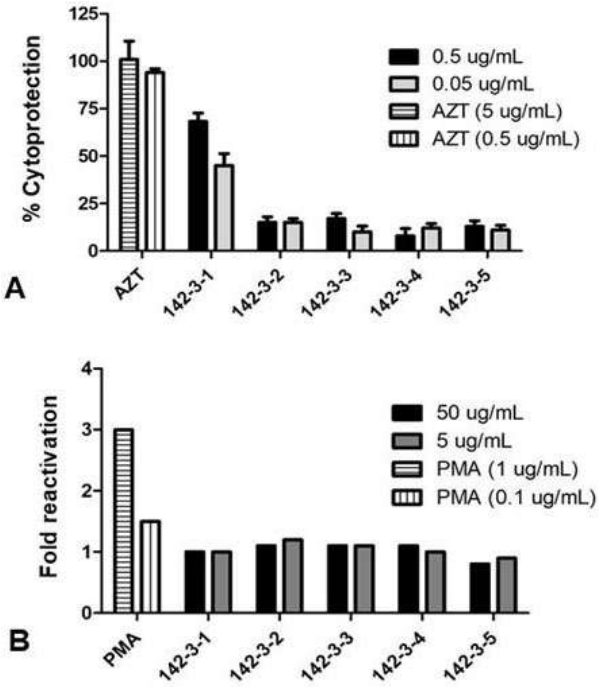

Figure IV. A – HIV cytoprotection assay results for the compounds 142-3-1 to 142-3-5. B – HIV latency reactivation assay results for the compounds 142-3-1 to 142-3-5.

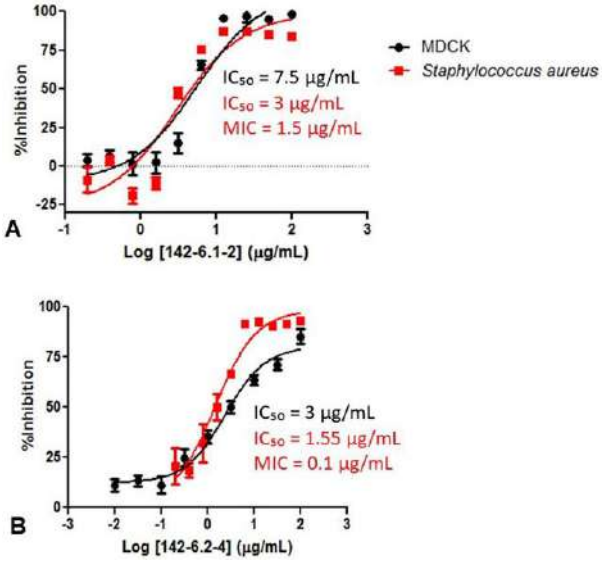

Figure V. Anti-*S. aureus* MDCK cytotoxicity of (A) 2-heptylquinolin-4-ol (Compound 2) and (B) 2-nonylquinolin-4-ol (Compound 3).

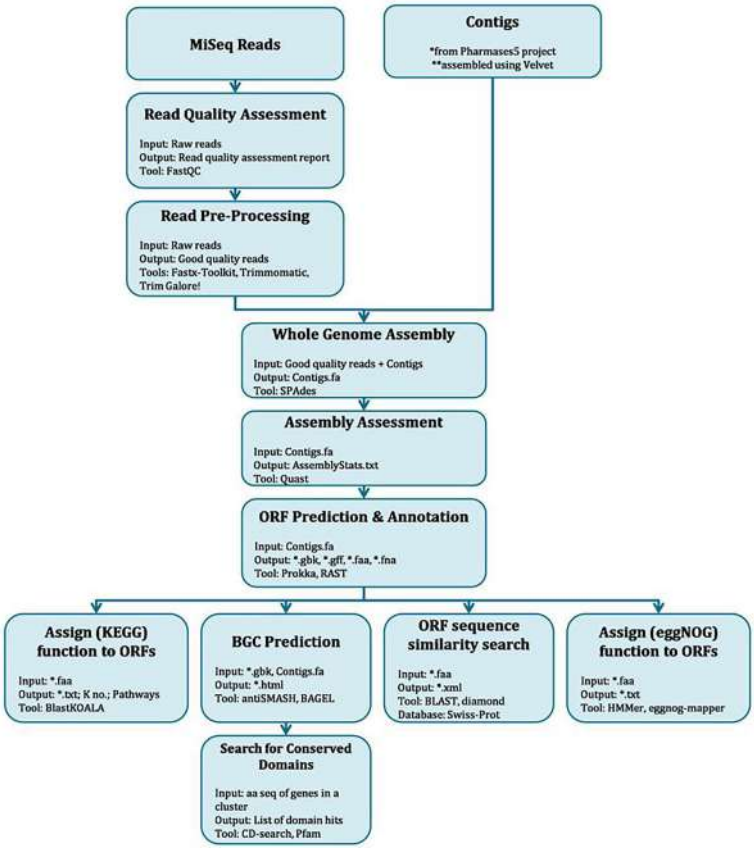

Figure VI. Genome assembly and annotation workflow for ISP2-142-O-2-A. The input and output files as well as the tools utilized per process are indicated.

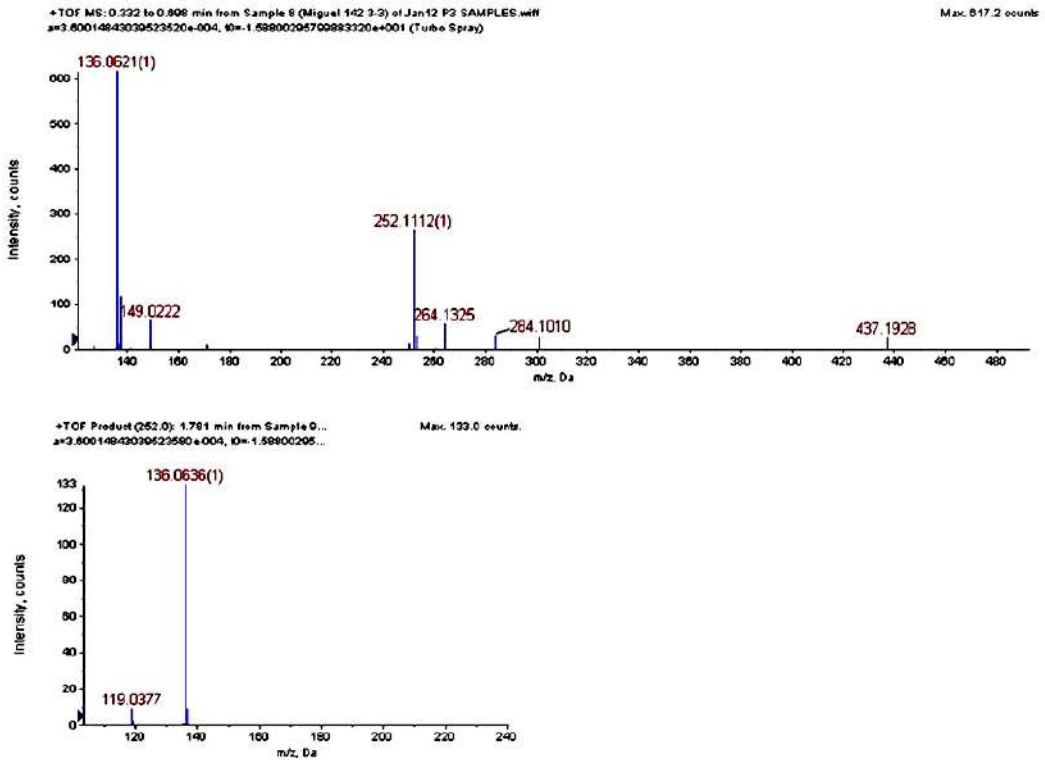

Figure VII. HRMS (above) and MSMS (below) spectrum of 5'-deoxyadenosine.

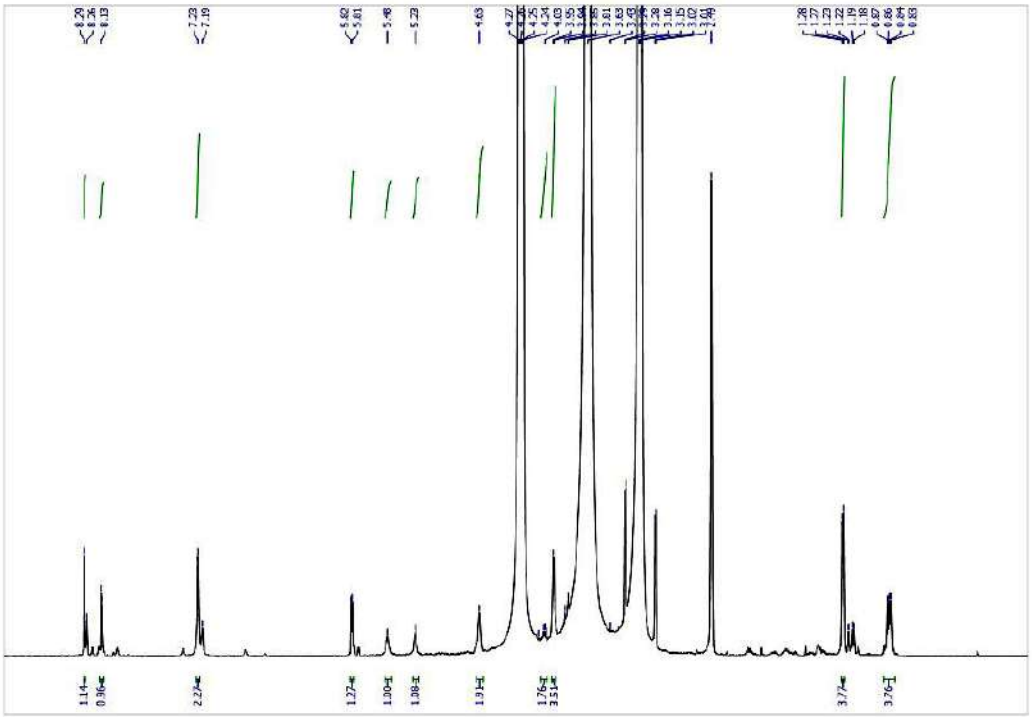

Figure VIII. ^{1}H NMR spectrum of 5'-deoxyadenosine.

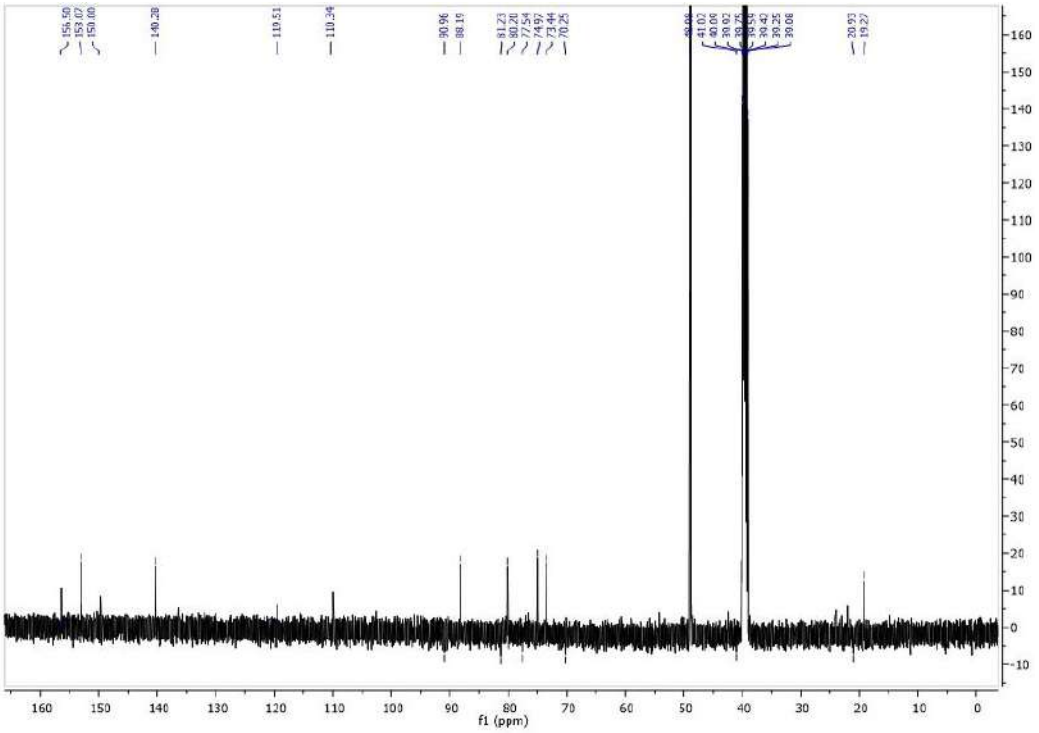

Figure IX. ^{13}C NMR spectrum of 5'-deoxyadenosine.

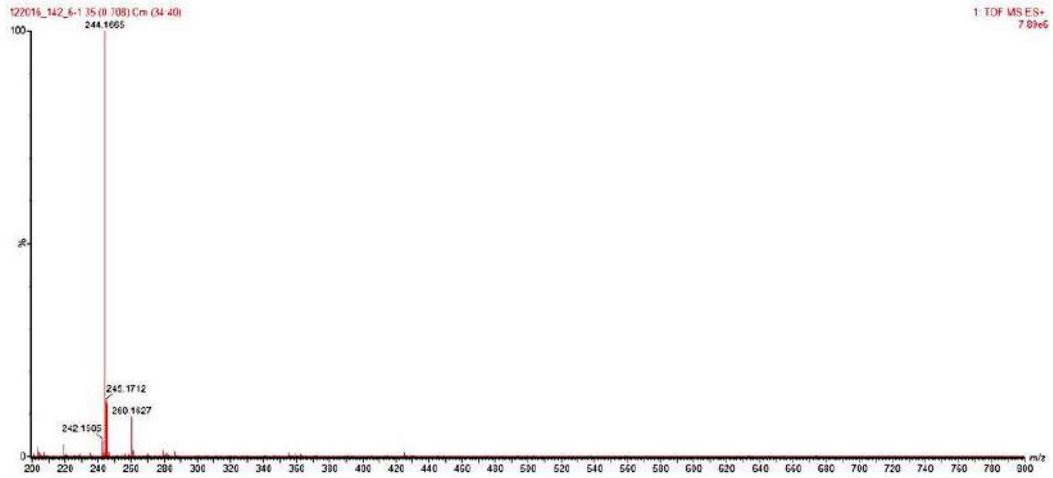

Figure X. HRMS spectrum of 2-heptylquinolin-4-ol.

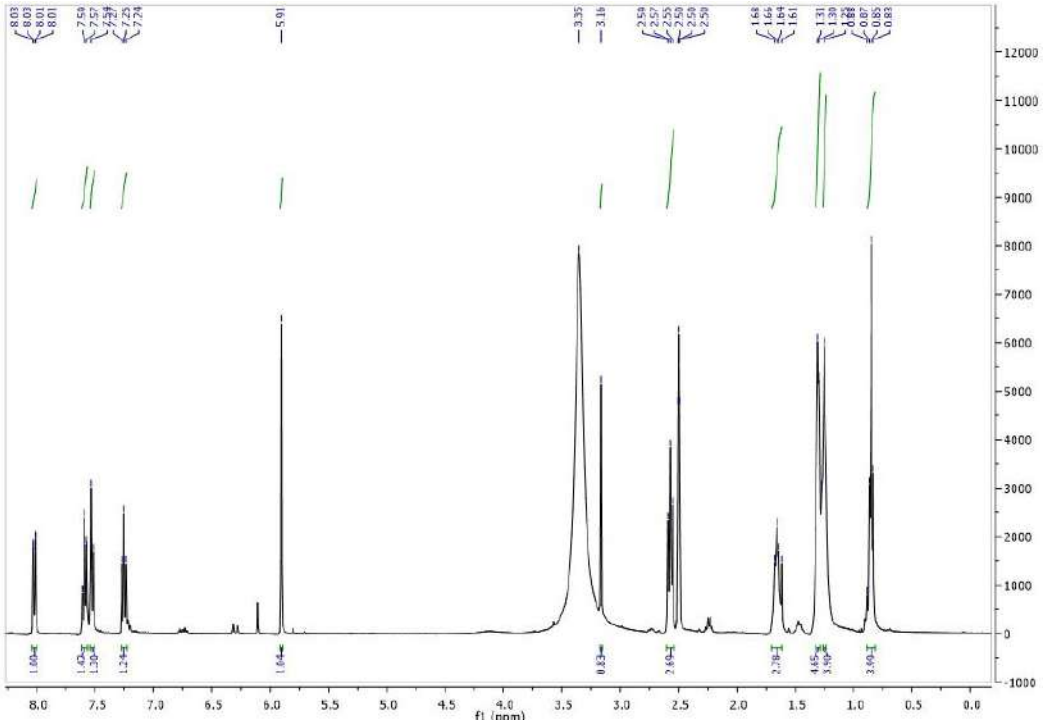

Figure XI. ^{1}H NMR spectrum of 2-heptylquinolin-4-ol.

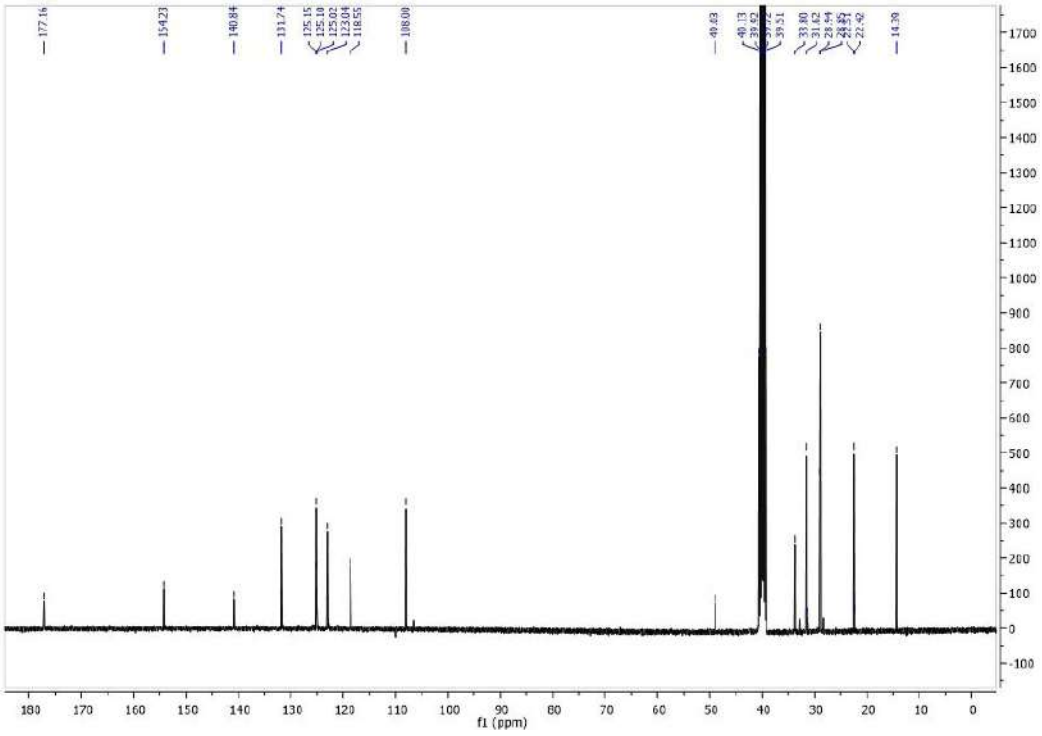

Figure XII. ^{13}C NMR spectrum of 2-heptylquinolin-4-ol.

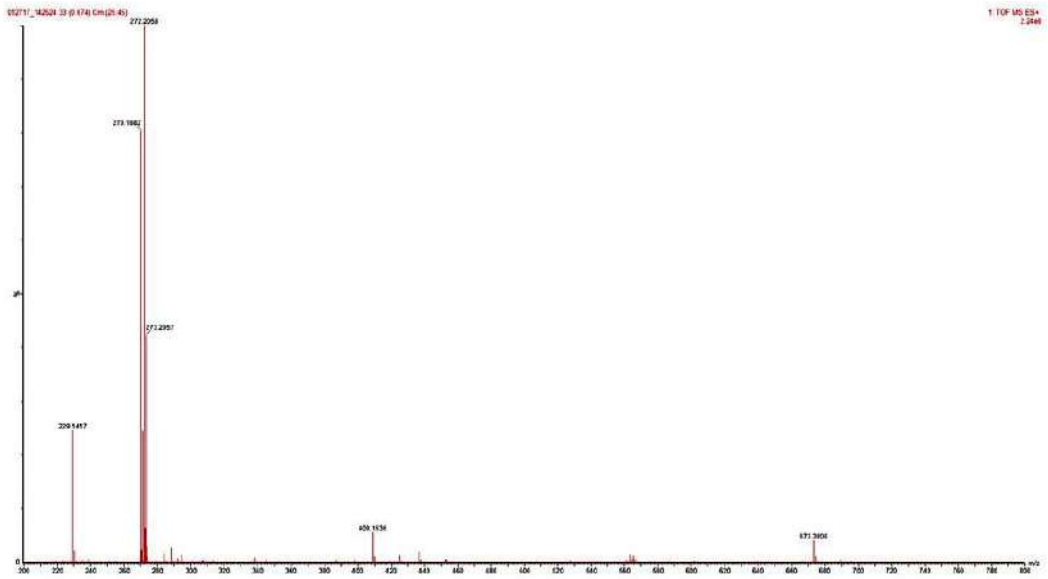

Figure XIII. HRMS spectrum of 2-nonylquinolin-4-ol.

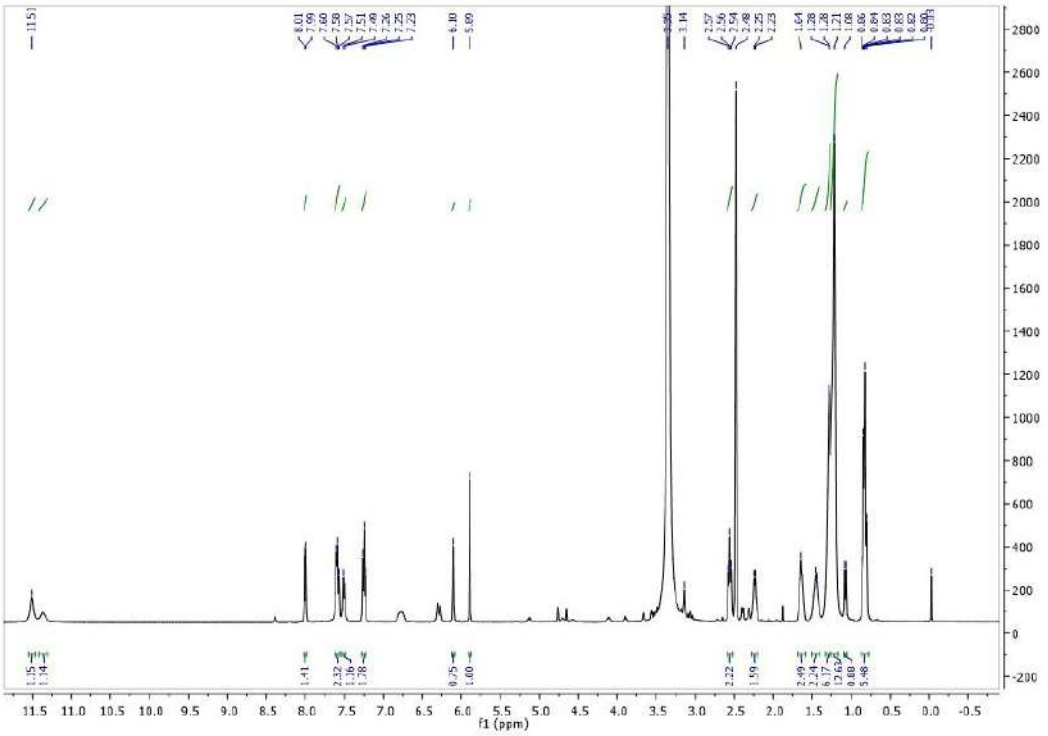

Figure XIV. ^{1}H NMR spectrum of 2-nonyl-quinolin-4-ol.

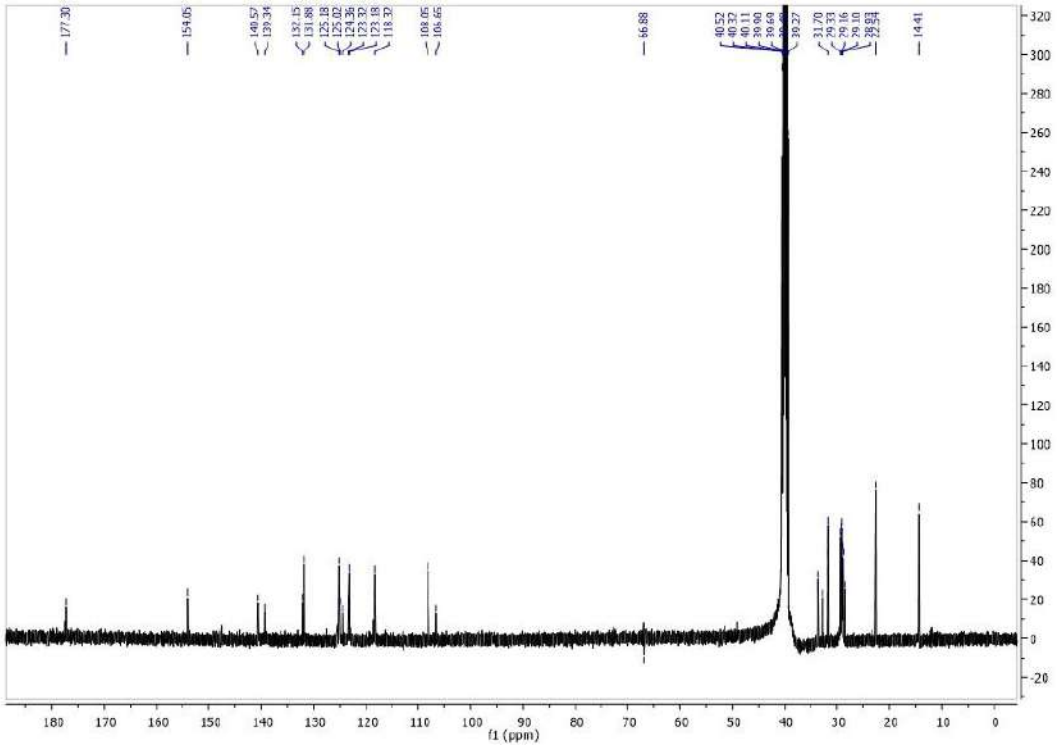

Figure XV. ^{13}C NMR spectrum of 2-nonylquinolin-4-ol.